

I.Mihai

Statistical tools for analysis of the performance

of a high resistance measurement bridge

R.T 05/2021

Marzo 2021

I.N.R.I.M. TECHNICAL REPORT

Abstract

The technical report exploits the use of Allan variances and the spectral power density to analyze the performance of the high resistance measurement Wheatstone modified bridge of commercial type.

The study was performed by observing the current measurements of the bridge detector as a function of its integration time. From a preliminary analysis of the data obtained, the main sources of noise of the system have been identified in correspondence with the integration times of the detector.

Sommario

Il rapporto tecnico descrive l'utilizzo delle varianze di Allan e della densità di potenza spettrale per individuare le sorgenti di rumore che si possono riscontrare nel funzionamento del ponte di Wheatstone modificato di alta resistenza di tipo commerciale. Lo studio è stato condotto osservando le misure di corrente del detector del ponte in funzione del tempo di integrazione del medesimo. Da un'analisi preliminare dei dati ottenuti sono stati individuate le principali sorgenti di rumore del sistema in corrispondenza dei tempi di integrazione del detector.

INDICE

	<i>page</i>
1. Introduction.....	4
2. Evaluation of the different type of noises.....	4
3. Analysis the data.....	9
4. High resistance measurement Wheatstone modified bridge.....	9
5. Results and discussion.....	16

Bibliography

1. Introduction

The technique of Allan variance and the power spectral density, familiar in the time and frequency metrology, has been successfully applied in order to improve the performance in resistance measurement systems and to solve the noise problems [1]. These tools have been used in the past by the author of this work to optimize a potentiometric measurement system and a bridge based on a cryogenic current comparator [2, 3]. As observed in this works, noise is an undesired parameter in sampling signals. It limits the attainable standard deviation of the estimated parameters, retrieved from sampled data. It is therefore important to know noise limitations of the sampler used for measuring sampled signal parameters at the lowest attainable uncertainties, which would be fundamentally limited by noise in the sampled signal. The data correlation due to $1/f$ noise has a great impact on measurement distribution and standard deviation. In particular, a series of non-correlated data, the distribution is characterized by the standard deviation of the mean. For correlated data, this statement is no longer valid. Measuring for any longer than the optimum measurement time for the measurement bridge is counterproductive, as the random drift will start to dominate. In addition, failure to correctly treat correlations can produce significant errors in any Type A uncertainty. One application of such evaluation concerns the measurement of standards resistors in the $T\Omega$ range with a Wheatstone modified bridge. The aim of this work is the identification of the white noise regime, by means of the mathematical estimators, in order to be used successively to carry out electrometer readings for the high value resistances of $10 T\Omega$, $100 T\Omega$ and $1 P\Omega$ in direct current with the modified Wheatstone bridge of a commercial type.

2. Evaluation of the different type of noises

As different types of noise exist in DC voltage sources, the standard variance is not a suitable statistic to describe the measurements stability. In this case it is better to analyze the measurements with the Allan variance. If the measurement data are independent, the Allan variance equals the standard sample variance [4, 5, 6, 7]. In addition, when a digital multimeter is used for sampling, different sources of noise are contributing to the total noise of the sampled signal.

2.1 Allan variances

For a signal sampled by a digital multimeter (DMM) at constant time intervals τ_0 the Allan variance $\sigma^2(\tau_0)$ is given by the equation [4]:

$$\sigma^2(\tau_0) = \frac{\langle (\bar{y}_{l+1}(\tau_0) - \bar{y}_l(\tau_0))^2 \rangle}{2} \quad (1)$$

where $\bar{y}_l(\tau_0)$ is the mean value in the l^{th} time interval and the angular brackets denote an infinite time average. It is also called the original non-overlapped Allan, or two-sample variance, AVAR. For a series of N measurements, sampled without death time, the Allan variance $\sigma^2(\tau_0)$ is given by:

$$\hat{\sigma}_y^2(\tau_0) = \frac{1}{2(N-1)} \sum_{l=1}^{N-1} (\bar{y}_{l+1}(\tau_0) - \bar{y}_l(\tau_0))^2 \quad (2)$$

To calculate the Allan variance as a function of the integration time τ new series of data are formed from the original set by grouping adjacent measurements, corresponding to time intervals $2\tau_0$, $4\tau_0$, $8\tau_0$, $16\tau_0$, $2^n\tau_0$ which generates n series of N_n measurements. The Allan variance as a function of the integration time, $\tau = 2^n\tau_0$ is:

$$\hat{\sigma}_y^2(\tau) = \frac{1}{2(N_n-1)} \sum_{l=1}^{N_n-1} (\bar{y}_{l+1}(\tau) - \bar{y}_l(\tau))^2 \quad (3)$$

where $N_n = \text{integer}(N/2^n)$.

The use of overlapping samples improves the confidence of the resulting stability estimate, but at the expense of greater computational time. The overlapping samples are not completely independent, but increase the effective number of degrees of freedom. The choice of overlapping samples applies to the Allan variances [5, 6]. Overlapping samples do not apply at the basic measurement interval, which should be as short as practical to support a large number of overlaps at longer averaging times.

$$\hat{\sigma}_y^2(\tau) = \frac{1}{2m^2(N_n - 2m + 1)} \sum_{j=1}^{N_n - 2m + 1} \left\{ \sum_{i=j}^{j+m-1} (\bar{y}_{i+1}(\tau) - \bar{y}_i(\tau)) \right\}^2 \quad (4)$$

where m is the averaging factor, as graphically explained in Figure 1.

Some stability calculations can utilize overlapping samples, whereby the calculation is performed by utilizing all possible combinations of the data set, as shown in Figure 1.

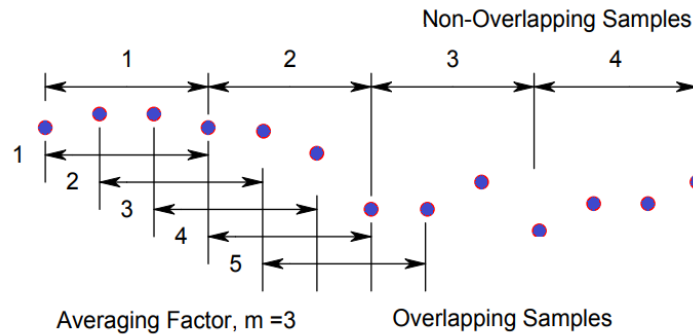


Figure 1. Comparison of different sampling.

The fully overlapping Allan variance, or AVAR, is a form of the normal Allan variance that makes maximum use of a data set by forming all possible overlapping samples at each averaging time τ . The confidence interval of an overlapping Allan deviation estimate is better than that of a normal Allan variance estimation because, even though the additional overlapping differences are not all statistically independent, they nevertheless increase the number of degrees of freedom and thus improve the confidence in the estimation. Analytical methods are available for calculating the number of degrees of freedom for an estimation of overlapping Allan variance, and using that to establish single- or double-sided confidence intervals for the estimate with a certain confidence factor, based on Chi-squared statistics. Sample variances are distributed according to the expression:

$$\chi^2 = \frac{\nu \cdot s^2}{\sigma^2} \quad (5)$$

where χ^2 is the Chi-square, s^2 is the sample variance, σ^2 is the true variance, and ν is the number of degrees of freedom.

For a particular statistic, ν is determined by the number of data points and the noise type. The equivalent number of χ^2 degrees of freedom associated with a statistical variance (or deviation) estimate depends on the variance type, the number of data points, and the type of noise involved. In general, the progression from the original two-sample Allan variance to the overlapping, variances has provided larger ν and better confidence. The noise type matters because it determines the extent that the points are correlated. Highly correlated data have a smaller ν than those with the same number of points of uncorrelated (white) noise.

2.2 Power spectral density

For the evaluation of the intrinsic noise of the DC current measured by the detector, an analysis of the power spectrum of the signal obtained by the detector readings is made with known resistors involved in the bridge arms using a DMM connected at the output of the detector D. The set of the two instruments, current detector and its output circuit, can be represented as a unidirectional system characterized by a transfer function H_D and an input signal $x(t)$. The output signal $y(t)$ is a convolution system of $x(t)$ and H_D .

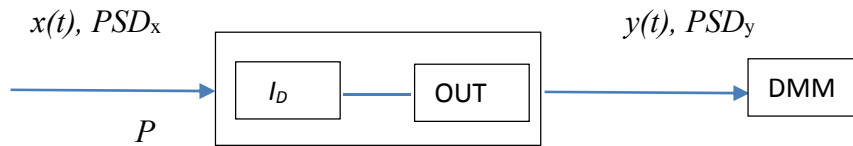


Figure 2. The system of the two instruments: a direct current detector and a DMM connected to its output.

The evaluation of the intrinsic noise of the DC sources can also be analyzed by means of the power spectral density. For a continues function $y(t)$, assumed to be periodical in the time interval t_T , the Direct Fourier Transfor (DFT) $F_y(f, t_T)$ is given by the equation [4, 5]:

$$F_y(f, t_T) = \int_0^{t_T} y(t) e^{-j(2\pi f t)} dt \quad (6)$$

The power spectral density $PSD(f)$ is given by the equation:

$$PSD_y(f) = \lim_{t_T \rightarrow \infty} \frac{2}{t_T} |F_y(f, t_T)|^2 \quad (7)$$

For the analysis of the power spectrum of the output signal $y(t)$, it is necessary to study the behavior of the $PSD_y(f)$ as a function of the frequency. The measurement unit for $PSD_y(f)$ is V^2/Hz . Usually a logarithmic representation is preferred for the both axes in order to observe the low frequency domain. In terms of the spectral power density, for the unidirectional system considered in Figure 2 can be written:

$$PSD_y(f) = |H_D(f)|^2 PSD_x(f) \quad (8)$$

The transfer function $H_D(f)$ is composed of the detector transfer function and its output circuit. This function depends on the RC low filter characteristics of the detector to its output.

The power spectral density $PSD_y(f)$ of a time series $\bar{y}_l(\tau_0)$ can be modelled according to the following power law:

$$PSD(f) = \sum_{i=-2}^2 \eta_i f^i \quad (9)$$

Where the intensity coefficient η_i and the index i depend on the type of noise.

The Allan variance $\sigma_y^2(\tau)$ and the power spectral density $PSD_y(f)$ corresponding to the three types of low frequency noise [1, 2] are presented in Table 1.

Table 1. Three types of low frequency noise.

Type	$PSD_y(f)$	$\sigma_y^2(\tau)$
white noise	η_0	$\eta_0/2\tau$
1/f noise	$\eta_{-1}f^{-1}$	$2\eta_{-1}\ln(2)$
Random walk noise	$\eta_{-2}f^{-2}$	$\frac{2}{3}\pi^2\eta_{-2}\tau$

In this table it can be observed that, in the case of white noise, the Allan standard deviation is proportional to $\tau^{-1/2}$. For random walk noise the Allan deviation increases with the square root of the integration time. The power spectral density is constant for white noise and is inversely proportional to the frequency for 1/f noise. The most common method for power law noise identification is simply to observe the slope of a log-log plot of the Allan or modified Allan deviation versus averaging time, either manually or by fitting a line to it. This obviously requires at least two stability points. For example, the thermal noise voltage at 23 °C and 1 Hz band for a 100 TΩ resistor, given by the RMS Johnson noise. It can be proven that the spectral power density, in case of thermal noise for an ideal resistors R, is $4k_BTR$ and is frequency independent (white noise). The terms k_B and T are respectively the Boltzman constant and the absolute temperature.

3. Analysis the data

For the entry, editing, simulation, analysis the data and the plotting it was used the free software program Stable32 and Microsoft Windows operation system. It is used by leading government and commercial metrology laboratories around the world, can be obtained free of charge from:

<https://ieee-uffc.org/frequency-control/frequency-control-software/stable32/>

This software is compliant with IEEE Std 1139-2008 – IEEE Standard Definitions of Physical Quantities for Fundamental Frequency and Time Metrology – Random Instabilities.

Stable32 file operations include opening data files, combining data, and storing all or a portion of the data. Data is stored in ASCII format, with gaps indicated by a value of zero, and may be input from any source that generates up to 8 columns of such comma or space-delimited data, with or without timetags. All storage and calculations of the equation are performed with double precision for a virtually unlimited number of data points. Plotting and printing can be done for all or a portion of the data, with drift fits and automatic or user-defined scales and titles. The more divergent noise types are sometimes referred to by their color. White noise has a flat spectral density (by analogy to white light). Flicker noise has an f^{-1} spectral density, and is called pink or red (more energy toward lower frequencies). Continuing the analogy, f^{-2} (random walk) noise is called brown.

Analysis functions include basic statistics, drift, drift removal, normalization, scaling, gap and outlier detection and removal, as well as Allan variance, histograms, and power spectrum, all over selectable limits with gaps ignored. Stability analysis includes point and automatic calculation and plotting of the normal and overlapping Allan deviation, PSD and other analysis as modified Allan deviation, ecc. Statistical techniques are available to estimate or define the noise type and to establish selectable confidence intervals. More details at free handbook from the web link.

4. High resistance measurement Wheatstone modified bridge

In the Wheatstone modified bridge a measurement consists of balancing of the bridge, followed by a waiting time for the stabilization and data acquisition from the current detector. At fixed voltage V_x , the voltage V_s is varied until the current reading of the detector I_D corresponds to the reading at zero

voltage ($V_x = V_s = 0$) measurements over the resistors under measurement R_x and standard resistor R_s . The measurement is repeated at reversed polarity of two DC voltage calibrators. The schematic principle of the bridge is shown in Figure 3.

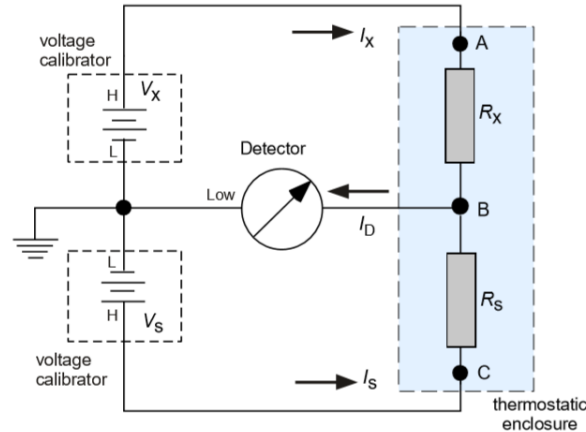


Figure 3. The principle of a Wheatstone modified bridge.

The low circuit impedance of the detector means that the current flowing in each resistor is determined by the voltage source effectively connected across it. The voltage ratio is set up such that these currents are in opposition and the detector measures the difference between these two currents. The mean detector reading is used to calculate a corrected final balance reading. The DC current I_D measured by the detector is given by sum of the currents flowing the arms of the bridge I_s and I_x :

$$I_D = I_s + I_x = \frac{V_s}{R_s} + \frac{V_x}{R_x} \quad (10)$$

The resistance ratio r is calculated as the ratio between the resistors under measurement R_x and standard resistor R_s at the condition $I_D \cong 0$:

$$r = \frac{R_x}{R_s} = -\frac{V_x}{V_s} \quad (11)$$

The value of the measurand R_x is obtained using the equation (11).

The measurement of the input current I_D is also subject to eddy currents, which are added to the input. For example, due to the triboelectric effect in the materials used for the connection cables, due to mechanical and electrochemical stress and due to the effect of the current generated on the bandwidth of the resistors due to their thermal noise.

4.1 Experimental system

The commercial measurement bridge, MI 6600A Automated Dual Source High Resistance Ratio Bridge (MI 6600A), has no battery powered electronics, and so is an ideal candidate for studying the Allan variance of the measurements, where very long acquisition times can be necessary. The commercial bridge consists of two model 1000C DC voltage sources that are programmable to 1000 V, an Input Signal Interface model MI 8100, and an electrometer / detector of type Keihley 6514 electrometer. Also the type Keihley 6517 electrometer measures the current difference flowing through the two resistors placed on the two active arms of the bridge. MI 6600A bridge is located inside a shield room in the laboratory Cp107 and it is connected independently to the ground potential. It is controlled by means of the IEEE488 interface bus connected to a personal computer from the outside the shielded room.

The flow diagram of a comparison between resistors at 1000 V is shown in Figure 6. The initial test predicts that, if after the first check of the unbalance window, the equilibrium is not obtained, the program repeats the measurement by doubling the initial value (in the case of this example 2 %). This is repeated three times after which, if there is still a balancing failure, the program stops and goes to Exit. If so, the program measures with positive polarity of V_x and subsequently, with reversed polarity. Measurements are stored and used for averaging. This method is used to eliminate the calibrator offset. The polarity is sequence a shown as in Table 2 in order to eliminate the effect of the thermal electromotive forces (emfs) by means of a polarity-reversing switch and the measurement repeated at reversed polarity of two DC voltage calibrators. A refinement of the method is to the alternative polarity reversal in such a way as to eliminate the effects of the emfs of the unreversed voltages [9, 10].

In the flow diagram, measurements consist of:

- a) the two resistors being measured,
- b) a settle time value,
- c) the number of electrometer/detector readings,
- d) the number of measurements being taken, and
- e) the number of readings to use when calculating statistics.

The desired settle time and electrometer readings must be selected from the pull down boxes along with the desired number of measurements (and statistics). The settle time may vary depending on the resistor being measured. The Unbalance Window determines at which current level the MI 6600A stops adjusting the voltage source when operating in bridge mode. This parameter is expressed in parts per million of the calculated full current readings flowing through one of the resistors. The minimum setting is 10 ppm or the equivalent calculation to 100 fA based on the measurement settings.

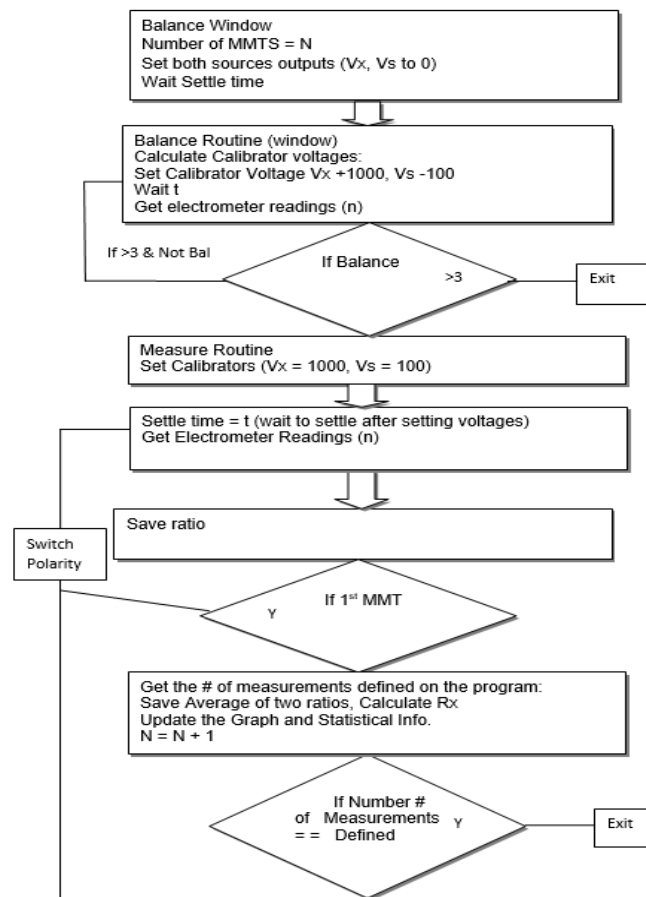


Figure 4. The flow diagram of a comparison between resistors at 1000 V and the ratio 10:1.

Table 2. Measurements as a cadence polarity reversal of the resistance ratio of equation (11).

Resistance ratio	Polarity reversal V_x	Results
r_{1p}	+ / p	r_{1p}
r_{2n}	- / n	$(r_{1p} + r_{2n})/2 = r_1$
r_{3p}	+ / p	$(r_{2n} + r_{3p})/2 = r_2$
r_{4n}	- / n	$(r_{3p} + r_{4n})/2 = r_3$
.....,,,
r_p	+ / p	$(r_{(i-1)n} + r_{ip})/2 = r_{i-1}$
r_n	- / n	$(r_{ip} + r_{(i+1)n})/2 = r_i$

Note: The meaning of index i is the progressive measurement resistance ratio. The index p and n are the positive, respectively, negative polarity. The polarity of voltage V_s is opposite to V_x .

The mean value of the resistance ratio \bar{r} at the end of the measurement session using the flow chart and the cadence polarity described before is given by:

$$\bar{r} = \frac{1}{N_r} \sum_{i=1}^N r_i \quad (12)$$

Where N_r is the number of the repetitions and r_i is the single measurement ratio obtained by the measurement bridge. So, the value of the measurand is: $R_x = \bar{r} \cdot R_s$.

The value of the device under test, the measurand, is always taken as the value extrapolated to complete stabilization, with no residual RC components in the measured signal [8, 9]. The electrometer/detector readings need to be carry out in the conditions of the white noise. During Voltage Polarity Reversal, the MI 6600A takes the average of two readings, one of each polarity, to calculate the resistor value. By doing this, possible offsets can be removed from the final result. From literature [4, 5, 6, 7, 8], precise measurements of DC voltage were made using a polarity reversal technique and the results were analyzed using the Allan variance in order to demonstrate that the polarity reversal is not sufficient to eliminate the 1/f noise. This is valid also when MI 6600A is operating in the bridge mode.

4.2 Current detector and the output circuit

The current detectors are widely used in national metrology institutes and calibration laboratories, where their sampling capability can perform highest accuracy low frequency measurements. This and other high accuracy measurement applications require a thorough understanding of their properties, among which noise performance is discussed.

For the experimental case, the bridge can be equipped by two current detectors to measure the current difference flowing through the two resistors: Keythley model 6514 or Keythley model 6517. They have a parabola-like shape for its speed vs. noise characteristics and are optimized for the readings rate between 16.67 ms and 166.67 ms. At these speeds, the detectors will make corrections for its own internal drift and still be fast enough to settle a step response. Some different technical characteristics are shown in Table 3.

Table 3. Comparisons between the technical characteristics of the Keithley detectors
(technical data from the operation manuals of the Keithley detectors).

Technical characteristics	6514	6517B
Resolution	100 aA	10 aA
(peak-to-peak) noise	< 1 fA	0,75 fA

The input current is converted to a voltage and supplied to the $2V$ output signal of the detector. Its provide a scaled $\pm 2 V$ that is inverting in the current mode measurement, as shown in Figure 5. Example of analog outputs are listed in Table 4.

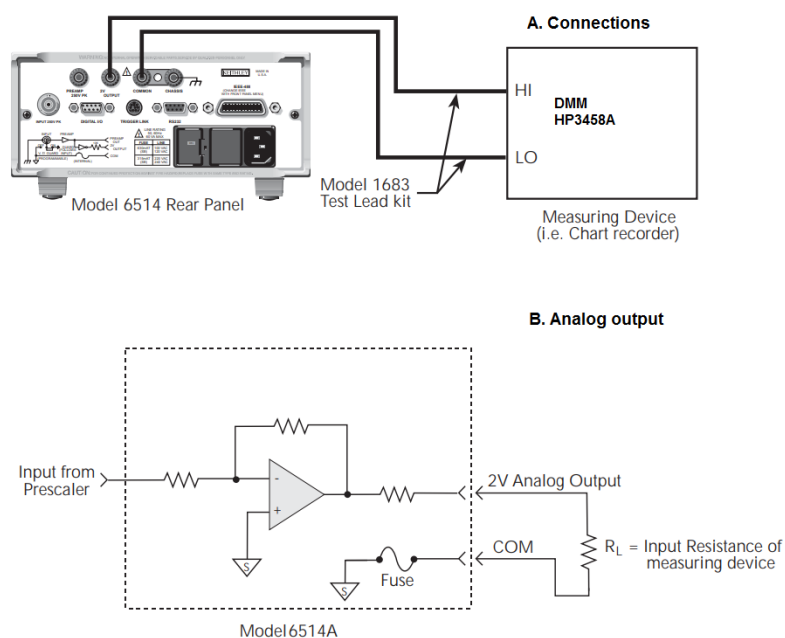


Figure 5. Output circuit to 2 V connection at the voltage input of a DMM (for example HP3458A).

Table 4. Example 2V analog output values

(technical data from the operation manuals of the Keithley detectors).

Range	Applied signal	Analog output value (nominal)
20 pA	10.5 pA	-1.05 V
2 μ A	-1.65 μ A	1.65 V

Another question arises of how to treat the correlation produced by the output low pass filtering, in order to get a reliable estimate standard deviation of the mean for the measurement, $\sigma(\overline{y(t)})$, where $y(t)$ is the electrometer/detector readings function.

In this case, standard deviation of the mean for the measurement is [7]:

$$\sigma^2(\overline{y_{\text{out}}}) \approx \frac{\sigma^2(y_{\text{out}})}{n} k \quad (13)$$

where, $k = \left[\frac{1+e^{-4B\tau_0}}{1-e^{-4B\tau_0}} \right]$ and y_{out} is the electrometer readings

Where B is the bandwidth of the low pass filter, τ_0 is the sample at equally time interval (time between readings) and $\sigma^2(y_{\text{out}})$ is calculated in the usual way for the set of n readings. In our case, for the experimental system described at the paragraph 4.1, $B\tau_0 \gg 1$. This means that the measurements are uncorrelated.

4.3 Digital sampling and acquisition software

The digital meter (DMM) noise specification is given in number of digits as a function of aperture time (T_a). This noise specification is referred to a resolution, the effective root mean square (RMS) noise of the whole instrument, represented as an effective noise referred to the input terminals. The DMM noise can be effectively measured with short-circuited input terminals when using double integer output format. Moreover, the DMM provides a state-of-the art accuracy for sampling low frequency signals. To minimize the effects of loading, the input impedance of the device connected to the *2V analog output* should be as high as possible. In case of the HP3458A, the manufacturer reports an input impedance greater than 10 G Ω for its 1 VDC function and for this reason it was used for the digital sampling, but also other DMM can be used. For the evolution of the intrinsic noise of the detector, an analysis of the voltage signal obtained at the output of the detector when two known resistors are connected at the bridge's terminal was made. The signal is measured by a DMM connected to the 2V output signal of the detector. The samples were taken automatically one after another using a "NRDGS 5000, AUTO" command. DMM was set to DINT output format using a "OFORMAT DINT" (command for $T_a > 1.4 \mu\text{s}$). All readings were transferred directly to the controller in real time using a Labview software, written on purpose for this work. Measurements

were performed using the short circuit across the input terminals at 100 Hz sampling frequency and 16.6 ms aperture time (as for the detector 6514). One segment with 16 384 samples taken at 100 Hz sampling frequency allows to analyze the power spectral density down to a few mHz, which is low enough to adequately capture the $1/f$ noise region. The samples were taken by reading samples directly by the GPIB controller.

5. Results and discussion

Using the electrometer/detector readings, obtained according to paragraph 4.3, and applying the software Stable32, the discussed mathematical estimators were calculated for two different setting of the ratio value R_x and standard resistor R_s , of 100 T Ω and, respectively, 10 T Ω (form MI, of the type 9331G):

1. The two resistors being measured, as in the case of no current supplied to the resistors since the voltage is not yet applied by the calibrators of the commercial bridge MI 6600A. In this case the detector readings I_D is null and is also a reference for the following measurements, as shown in Figure 4. The detector readings I_D correspond to the reading at zero voltage ($V_x = V_s = 0$); The measurements are saved in the file *Allan_senza_tensione.txt*.
2. The two resistors being measured, at the voltage test $V_x = 1000$ V and respectively $V_s = -100$ V, as in the case of *Unbalance Window* at the minimum setting of 10 ppm. In this case the detector readings I_D is also near zero. The spectra of these readings should as close as possible to the previous condition. The measurements are saved in the file *Allan_con_tensione_1000V.txt*.

The preliminary results of the analysis performed by means of these mathematical estimators applied to both experimental cases are graphically shown in the Figure 6 and, respectively, Figure 7.

In Figure 6. a) and b) for the first experimental case (no current is supplied to the resistors), the mathematical estimators show a behavior as close as a white noise regime because the Allan standard

deviation and Overlapping Allan Deviation are proportional to $1/\tau$ (until 300 s for the Overlapping Allan Deviation) and the data are not correlated.

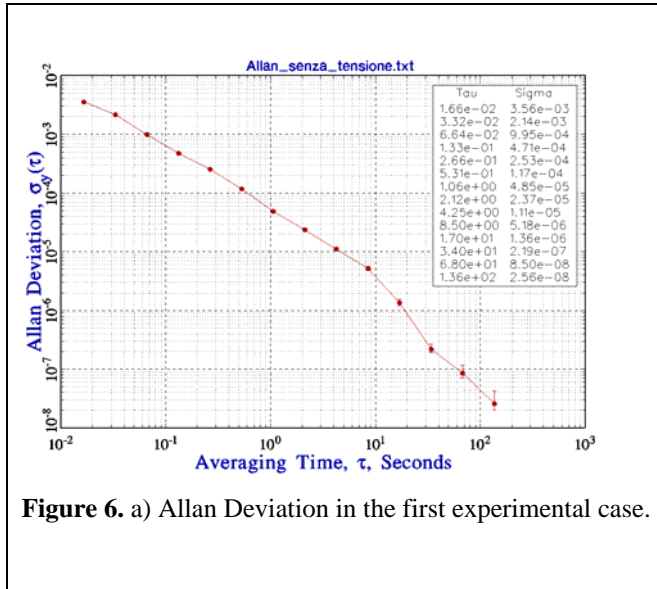


Figure 6. a) Allan Deviation in the first experimental case.

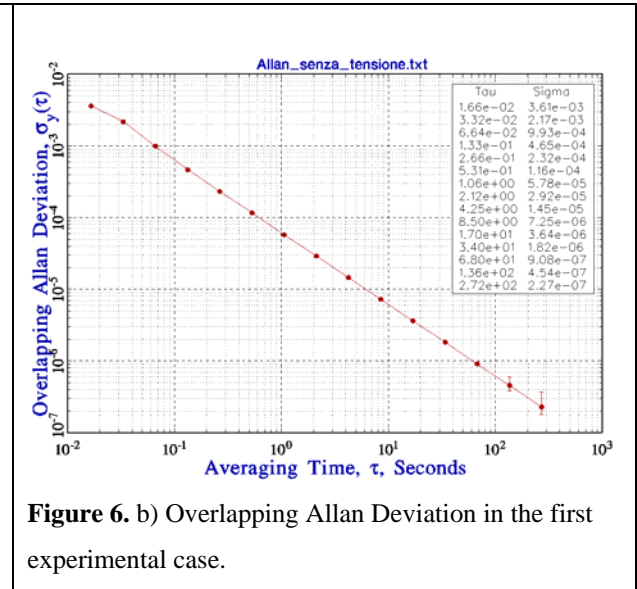


Figure 6. b) Overlapping Allan Deviation in the first experimental case.

In the second experimental case, plotted in the Figures 7. a) and b), the mathematical estimators show a behavior which is not characteristic of the white noise, and this should be analyzed in order to operate the measurement system in better conditions. If the data are correlated the behavior of the Allan deviation is flat. The power spectral density in the second case of study (at the voltage test $V_x = 1000$ V and respectively $V_s = -100$ V) as shown in Figure 7. c), is a combination of several types of noises, and this is an evidence of some correlation between the measurements.

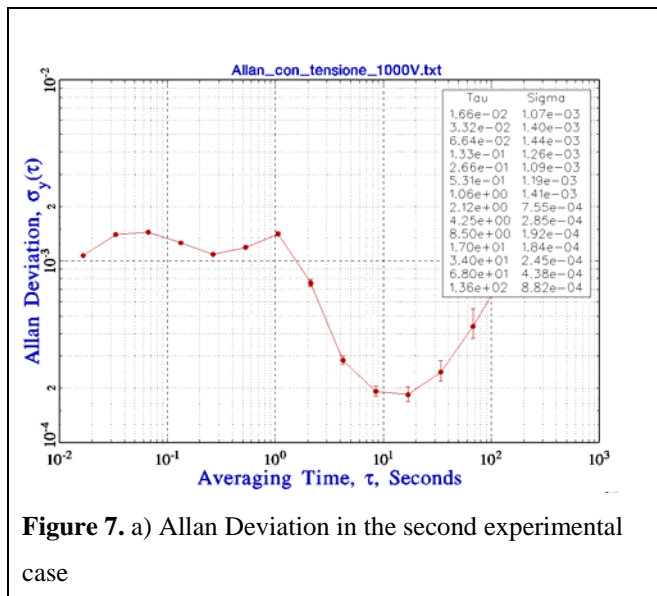


Figure 7. a) Allan Deviation in the second experimental case

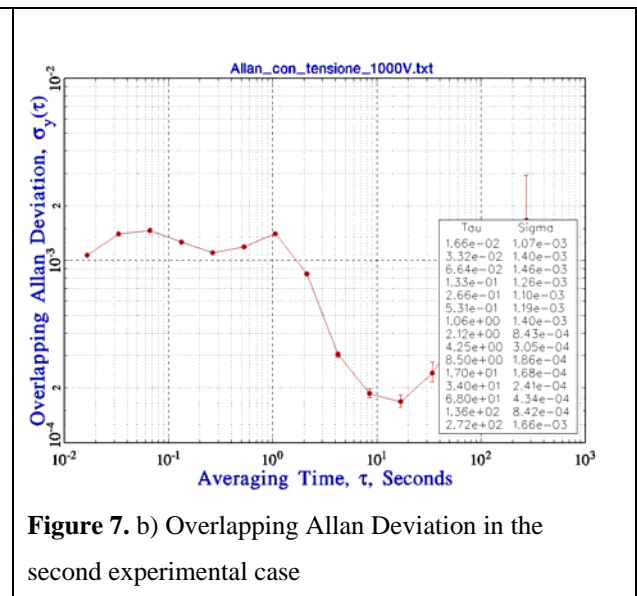


Figure 7. b) Overlapping Allan Deviation in the second experimental case

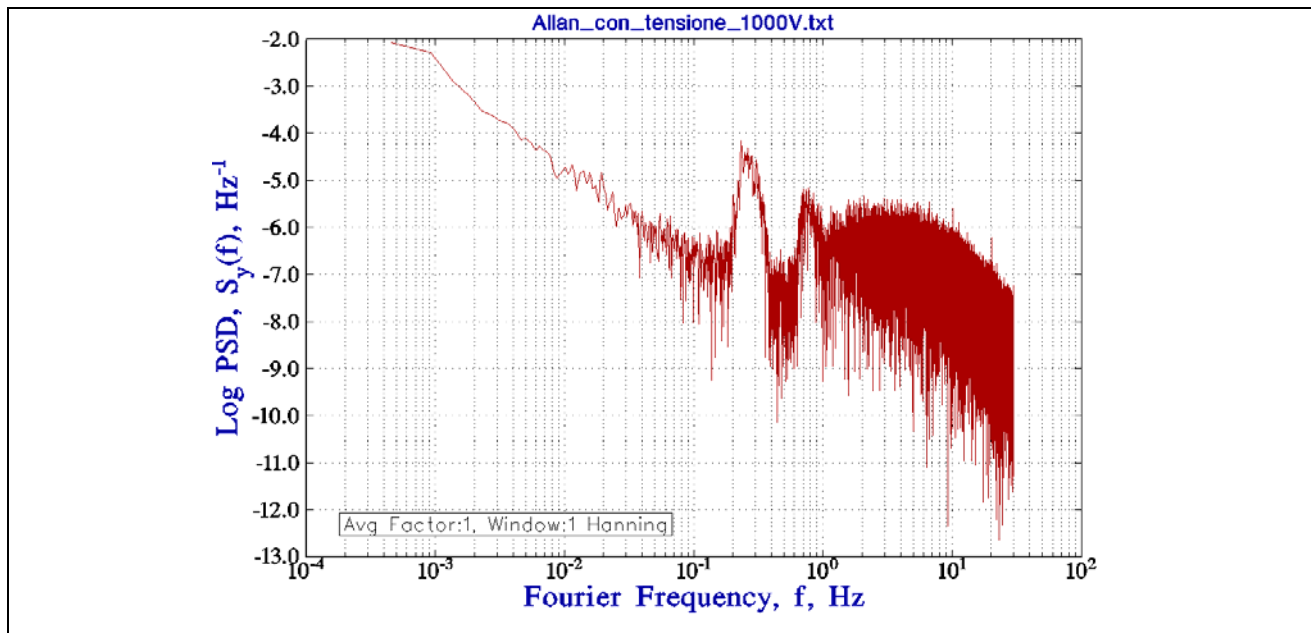


Figure 7. c) Power spectral density in the second experimental case.

Under condition with voltage at 1000 V and, respectively, at – 100 V the 1/f noise appears at short integrating time and the standard deviation reach its minimum value at about 20 s. Increasing integration time value does not reduce any more the standard deviation. Furthermore, this behavior can be attributed to the long time of the stabilization due to the residual RC components in the measured signal and this it is also a parameter that needs to be optimized and reduced to about 200 s. The data correlation due to 1/f noise has a great impact on measurement distribution and standard deviation. In particular, for a series of non-correlated data, the distribution is characterized by the standard deviation of the mean. For correlated data, this statement is no longer valid.

Measuring for any longer than the optimum measurement time for the measurement bridge is counterproductive, as the random drift will start to dominate.

In addition, failure to correctly treat correlations can produce significant errors in any Type A uncertainty.

Then the author of this work suggests setting the commercial bridge, for this ratio at 1000 V with this integration time in order to optimize the electrometer/detector readings. Future aim will be to investigate optimal conditions for other resistance ratios by means of the same estimators.

In conclusion, this report demonstrates some of the power and wide applicability of the analysis methods in order to optimize the electrometer/detector readings obtained by means of a Wheatstone modified bridge for each single ratio. Some of these advantages consist in reducing the loss time, revealing the presence of stochastic correlations in DC electrical measurement and quantifying measurement uncertainty in the presence of not-deterministic correlations of the electrometer/detector readings.

These technique will be used for different resistance ratio and different voltages in order to optimize the commercial bridge MI 6600A and reach its minimum uncertainty of type A, according to our quality system requirements.

Acknowledgement

I thank my colleagues Francesca Romana Pennechi and Giorgio Brida for their help with statistics and suggestions about the use of the free software program Stable32. In addition, I would like to thank to Flavio Galliana for his advises with high resistance measurement bridges and to Luca Callegaro for some constructive discussion and suggestion about using these classic statistical tools, described in this work, and other new tools.

Also, very significant to me, I would like to thank for the editorial suggestions proposed for this work by Pier Paolo Capra and Michela Sega.

Bibliography

- [1] T. J.Witt, “Using the Allan variance and power spectral density to characterize DC nanovoltmeters,” *IEEE Trans. Instrum. Meas.*, vol. 50, no. 2, pp. 445–448, Apr. 2001.
- [2] I. Mihai and G. Marullo Reedtz, “Using spectral analyses and Allan variance to characterise a potentiometric measurement system,” Proc. of the International Metrology Conference, Bucharest, pag. 555-560, 2001.
- [3] I. Mihai, G.Marullo Reedtz “Optimisation of a potentiometric measurement system by calculation of the Allan variance”, pp. 48-49. In. Prec. Elec. Measur. (CPEM) Digest, June 2002.
- [4] T. J. Witt, “Allan Variances and Spectral Densities for DC Voltage Measurements with Polarity Reversals, *IEEE Trans. Instrum. Meas.*, vol. 54, no. 2, pp. 550–553, 2005.

- [5] T. J. Witt, “*Investigations of Noise in Measurements of Electronic Voltage Standards*”, *IEEE Trans. Instrum. Meas.*, vol. 54, no. 2, pp. 567 - 570, 2005
- [6] T. J. Witt, “Using the autocorrelation function to characterize time series of voltage measurements”, *Metrologia*, 44 pp. 201-209, 2007
- [7] N. Fletcher, T.J.Witt, “Some applications of times series analysis techniques to coaxial ac bridges”, *Precision Electromagnetic Measurements Digest*, 2008. CPEM 2008
- [8] S. Hongwei, Li Yuli, Chen Guangfeng Xi’ “*Relations between the Standard Variance and the Allan Variance*” *IEEE Trans. Instrum. Meas.* 17-19 Dec. 2010
- [9] F. Galliana, P. P. Capra, I. Mihai “*Measurement comparison between a commercial high resistance bridge and validated systems at ultra-high resistance values*” IMEKO TC-4 2020 Palermo, Italy, September 14-16, 2020.
- [10] I. Mihai, F. Galliana “*Ponte automatico per elevate resistenze in corrente continua MI 6600A: modalità di utilizzo ed approfondimento delle condizioni di misura*” RT02/2021